# Radio Source Spectra and Structure: RATAN–600 and VLBA Observations

Yuri Y. Kovalev, Yuri A. Kovalev, Nikolai A. Nizhelsky

*National Radio Astronomy Observatory, Lebedev Physical Institute, Special Astrophysical Observatory*

## Abstract

We are using the RATAN 600 meter ring transit radio telescope near Zelenchukskaya, Russia, to observe the time variation of the radio spectra of quasars and AGN at 6 frequencies over the range 1 to 22 GHz. The RATAN data, which covers the period 1995–2003 with 2 to 4 observations per year, are compared with 15 GHz VLBA observations of the milliarcsecond source structure (Kellermann et al. 1998, Zensus et al. 2002). Many sources show pronounced spectral variability with observed flux density changes of up to an order of magnitude over a period of a few years. Observations made only a few years apart often show very different types of spectra. Comparison of the VLBA images with the total power RATAN data indicates that typically 70% to 100% of the total flux density is contained in the VLBA image. Most spectra are dominated by a single high frequency component which is thought to be a compact relativistic jet.

## Observations

In this work we have used monitoring data obtained up to 2002 for about 160 quasars and active galactic nuclei. Broad-band spectra observations were made at 31, 13, 7.7, 3.9, 2.7, and 1.4 cm, simultaneously for all frequencies, with the 600-m ring radio telescope RATAN–600 in the framework of a long-term monitoring program. Results of the observations made in 1997, December, list of the sources included in the monitoring, description of a method of observations and data processing are presented in Kovalev et al. (1999). Horizontal localization of the stationary antenna horns allows broad-band spectral responses to be obtained at all observed frequencies in a time of 1–2 minutes in the transit mode of meridional observations. VLBA data are obtained in the 2 cm VLBA monitoring program (see for details Kellermann et al. 1998, Zensus et al. 2002, as well as http://www.cv.nrao.edu/2cmsurvey/). RATAN–600 instantaneous spectra and VLBA 2 cm images for all the program sources may be found at the web site.

## Variable Radio Spectra

From statistical and numerical model analysis of observed spectra we conclude that the spectra can be modeled as the sum of a synchrotron spectrum of an extended optically thin component (magnetized envelope/lobe, 'spectrum 1'), dominating at lower frequencies, and a synchrotron spectrum of a compact component (relativistic jet, 'spectrum 2'), dominating at higher frequencies. Spectrum 1 is generally constant or weakly variable, spectrum 2 can exhibit any degree of variability. In Figure 1 we present examples of fitting the sum of spectra 1 and 2 (with different contributions to the total emission) to the RATAN observational data. The data at 5 and 2.7 GHz (for 0312+10), 1.4 GHz and bellow 1 GHz are taken from the CATS database (Verkhodanov et al. 1997). The model of a quasi-stationary jet in the longitudinal magnetic field is adopted for spectrum 2 (Nesterov et al. 1994). For the quasar 0552+39, the contribution of spectrum 1 is small or even negligible; next are the quasar 0923+39, the quasar 0838+13, and the galaxy 0312+10, successively by increasing the contribution of spectrum 1. Considering non-stationary jets, a combination of two spectral components can explain the features of spectra with complex shapes (Figure 2, 3). A variable emission of a jet can be produced by the non-stationary outflow of relativistic particles in the longitudinal magnetic field (see e.g., Kovalev et al. 2000) or by the propagation of relativistic shocks (see e.g., Marscher & Gear 1985).

Factors of cm flux density variations ranges from 1 to 15. Examples of spectra variability are presented in Figures 2, 3. A typical behavior of spectra evolution during strong radio outbursts is recognized: a wave of a perturbation moves along the spectrum from higher to lower frequencies (Figure 2). Quasars and BL Lacertae objects have similar fashion and rate of long-term variability. Therefore, the hypothesis of the same physical nature of flares in quasars and BL Lacs is supported. Objects of other type of variability were also observed. Spectra of two of them, 1034–29 & 1519–27, are displayed at the bottom of Figure 3. Variability features of these objects are explained by interstellar scintillations (see Macquart et al. 2000).

## Comparison with the VLBA Data

Figure 4 presents the distributions of the filled aperture $S_{\rm fa}$ (RATAN) and VLBA CLEAN total $S_{\rm tot}$ flux densities and their ratio (or "index of compactness"). The good correlation between $S_{\rm tot}$ and $S_{\rm fa}$ indicates that for most sources the VLBA sees nearly all of the flux density, and that there are no significant systematic errors in the flux density scale of the VLBA. Aside from the few sources that clearly have large scale structure, the mean compactness index $< S_{\rm tot}/S_{\rm fa} >$ for the sample is about 0.86. Several objects have a compactness index $S_{\rm tot}/S_{\rm fa} > 1$; most likely, this is due to the source variability and the non-simultaneity of the VLBA and filled aperture observations. Sources with the compactness index $S_{\rm tot}/S_{\rm fa}$ close to 1 at all epochs are suitable for calibration of other cm VLBI experiments.

The peak of $S_{\rm fa}$ distribution corresponds to the selection limit of the sample. The peak position and the shape of the left wing reflect the discrepancy between the actual 15 GHz flux density and the value estimated from extrapolation by Kellermann et al. (1998) and Zensus et al. (2002), largely due to the variability of the sources.

On modeling the broad band radio spectra of compact extragalactic radio sources, we derived that a compact relativistic jet must be responsible for the centimeter and millimeter part of the spectrum. It is also supported by the compactness analysis. Consequently, a correlation of a long term variability between $S_{\rm tot}$ and $S_{\rm fa}$ was anticipated. A check on its presence gave us a positive answer (see examples on Figure 5). These results confirm our previous interpretation of (i) quiescent spectra by the emission of a jet in a quasi-stationary phase and (ii) the spectra variability at frequencies higher than 1 GHz by the strongly variable spectrum 2.

Radio sources with average 11-22 GHz two-point spectral index $\alpha > -0.5$ ($S_\nu \sim \nu^\alpha$) display VLBI jet component motions with speeds in the range from $0c$ to about $30c$, while for sources with steeper spectra speeds not more than $6c$ are observed (Kellermann et al., in preparation).

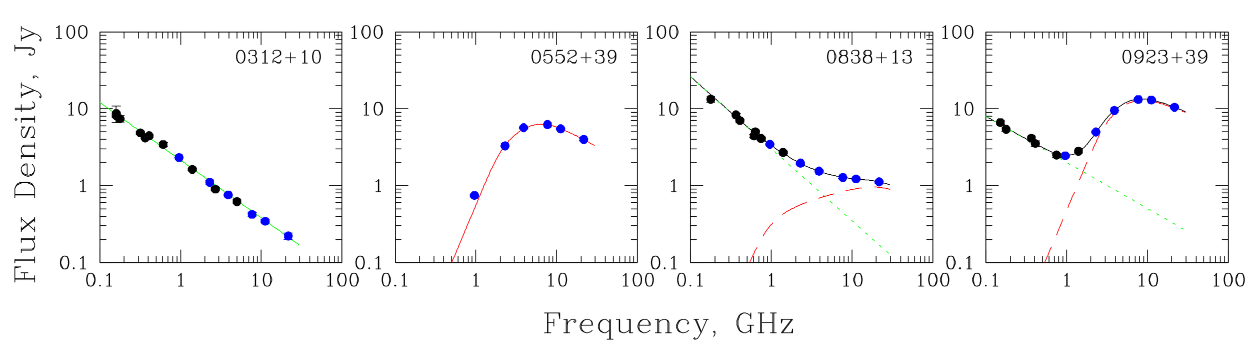


**Figure 1.** Examples of the model spectral fits. Total spectrum (blue) is the sum of a spectrum (green) of an extended optically thin component (magnetized envelope/lobe), constant or weakly variable and dominating at lower frequencies, and a spectrum (red) of a compact component (relativistic jet), dominating at higher frequencies, with any degree of variability. Errors are smaller than the point size when they are not visible.

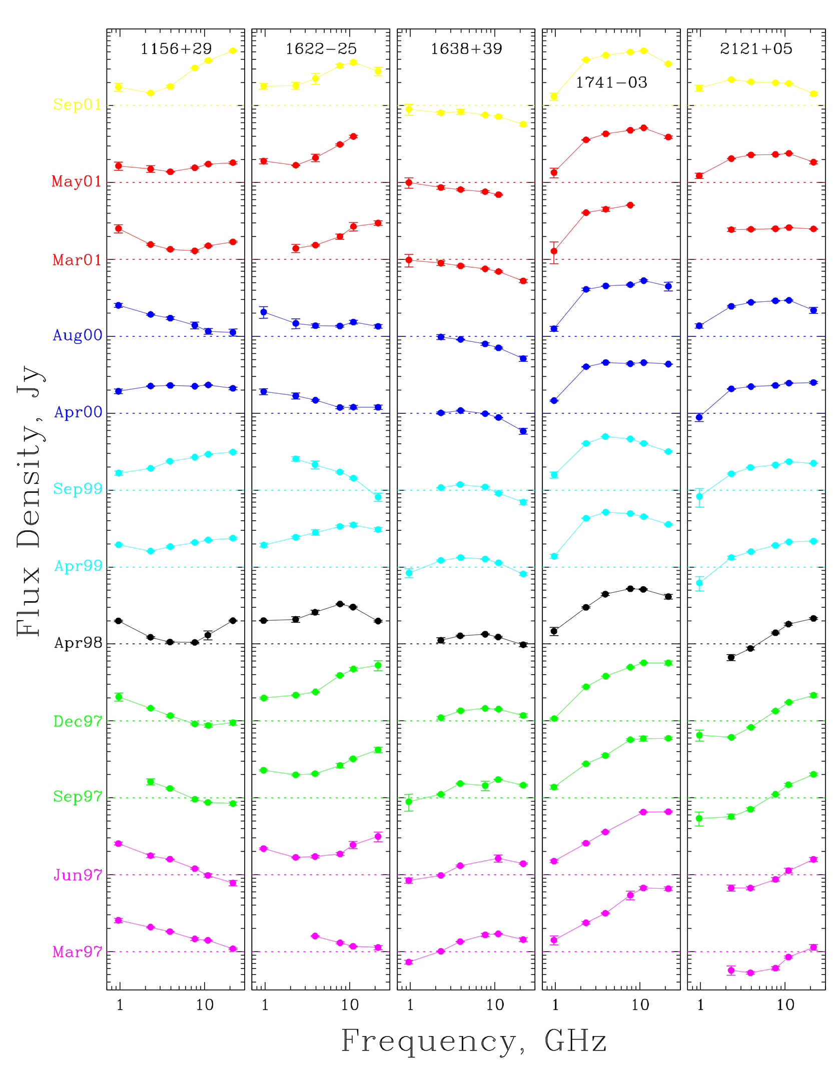


**Figure 2.** Examples of strong long-term variability of broad-band instantaneous spectra in 1997–2001. Evolution of the spectra is shown. Spectra for different epochs are given along the hight of the boxes. Dotted horizontal lines mark 1 Jy levels for each epoch. The spectra for these sources among others are presented in Figure 3 without shifting. An error is smaller than the point size when an error bar is not visible.

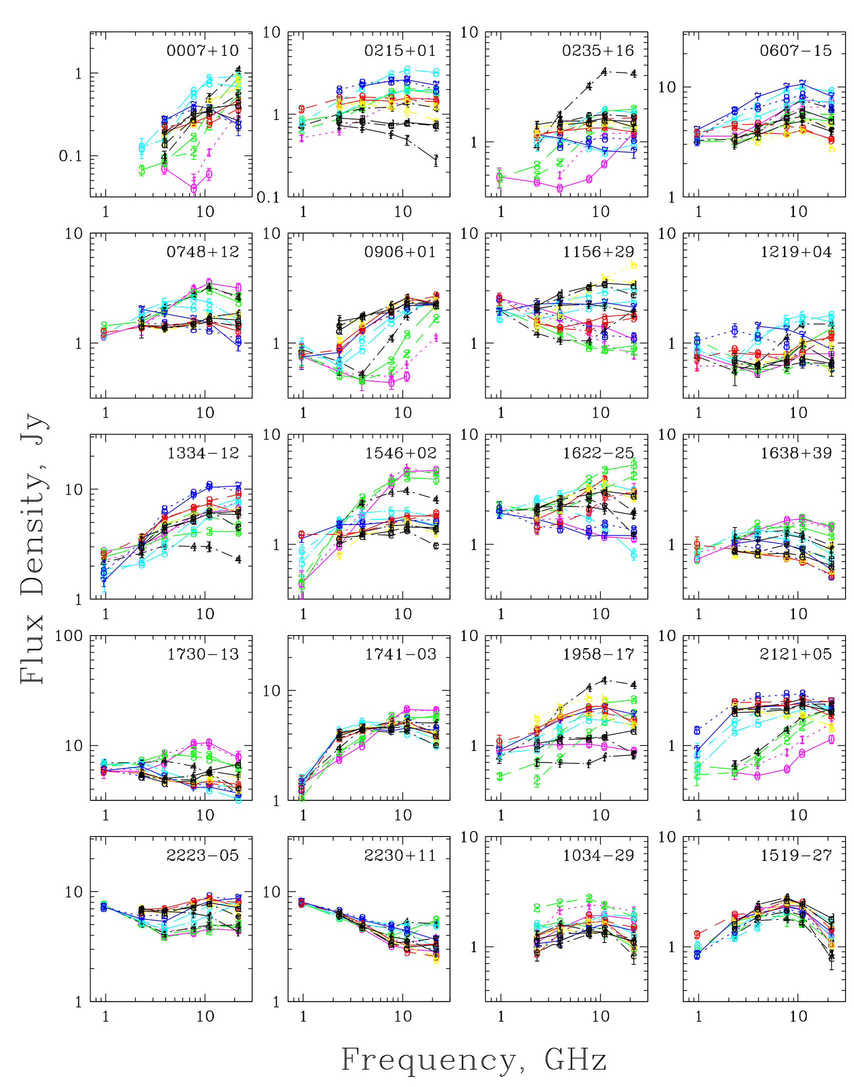


**Figure 3.** Examples of strong long-term variability of broad-band instantaneous spectra. Shown are the multi-epoch 1–22 GHz spectra for 1997–2002.

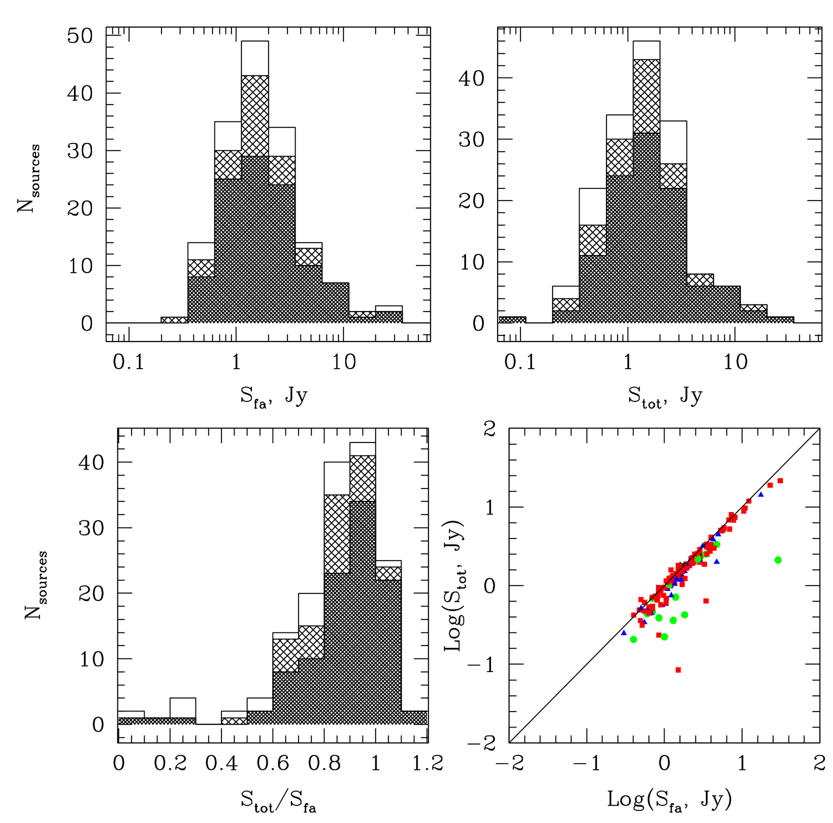


**Figure 4.** Source distributions on 15 GHz flux densities $S_{\rm fa}$ (RATAN), $S_{\rm tot}$ (VLBA total CLEAN), index of compactness $S_{\rm tot}/S_{\rm fa}$ and $S_{\rm tot}$–$S_{\rm fa}$ dependence (quasars are red, BL Lacs — blue, radio galaxies — green). We separate in histograms quasars (most hatched area) from BL Lacs (medium hatched) and active galaxies (empty).

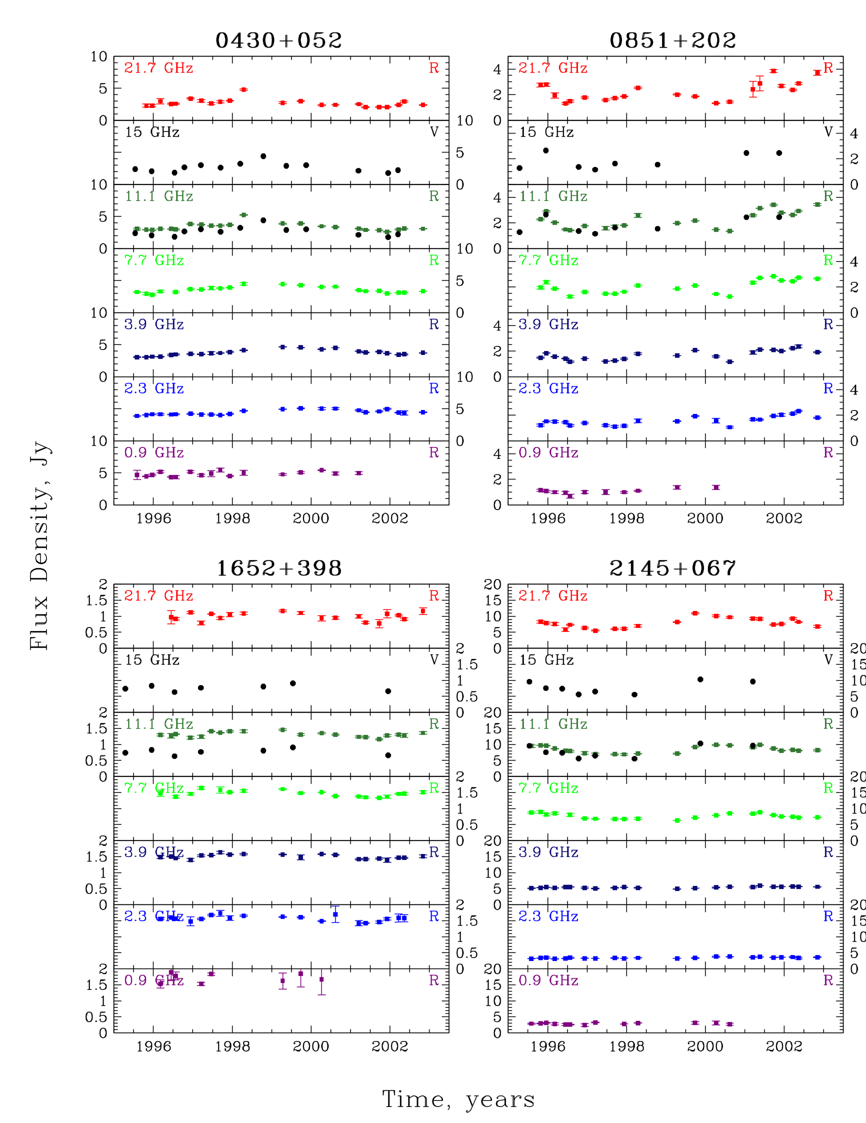


**Figure 5.** Example of light curves for RATAN (boxes marked 'R') and VLBA total CLEAN (boxes marked 'V') flux density data. VLBA points (black) are plotted also in the 11 GHz RATAN box for comparison.

This paper is based in part on work done in collaboration with M. H. Cohen, D. C. Homan, K. I. Kellermann, M. L. Lister, E. Ros, R. C. Vermeulen, J. A. Zensus, M. F. Aller, and H. D. Aller. The NRAO is a facility of the NSF operated under cooperative agreement by Associated Universities, Inc. We have made use of the database CATS (Verkhodanov et al. 1997) of the Special Astrophysical Observatory. This work has been partly supported by the NASA JURRISS program (W–19611).

**References**

Kellermann, K. I., Vermeulen, R. C., Zensus, J. A., & Cohen, M. H. 1998, AJ, 115, 1295
Kovalev, Y. Y., et al. 1999, A&AS, 139, 545
Kovalev, Yu. A., Kovalev, Y. Y., and Nizhelsky, N. A. 2000, PASJ, 52, 1027
Macquart, J.-P., Kedziora-Chudczer, L., Rayner, D. P., and Jauncey, D. L. 2000, ApJ, 538, 623
Marscher, A. P., and Gear W. K. 1985, ApJ, 298, 114
Nesterov, N. S., Kovalev, Y. Y., Babak, S. V., and Larionov, G. M. 1994, ARep, 38, 757
Verkhodanov, O. V., Trushkin, S. A., Andernach, H., and Chernenkov, V. N. 1997, ASP Conf. Ser., 125, 322
Zensus, J. A., et al. 2002, AJ, 124, 662